APCC
APEC CLIMATE CENTER

RESEARCH REPORT

APCC
APEC CLIMATE CENTER

PREFACE

It is our pleasure to present this report on the APEC Climate Center (APCC)'s research activities in 2013, which has been a very productive year for our Center.

APCC has expanded its research scope, in response to regional societal and scientific needs. While building expertise in climate prediction remains a priority, we are extending our reach to include policy-relevant climate applications and value-added climate information products.

APCC has accelerated efforts to better our service to the region. As one of the main services provided by APCC, the MME 3-month prediction information has been productively applied by scientists in developing countries that are unable to produce their own prediction information. Furthermore, in order to better prepare for climate-related hazards in a timely manner, APCC launched its 6-month MME prediction service in September 2013. We also began to release forecasts of the Boreal Summer Intraseasonal Oscillation (BSISO), starting from July 2013, as the world's first operational BSISO forecast service. Our researchers also achieved great success in publishing their papers in noted academic journals. Dr. Ok-Yeon Kim, for example, published a paper in *Climate Dynamics* and her research was later selected as one of the Research Highlights by another distinguished journal, *Nature Climate Change*. The following research report provides more information about our research outcomes from 2013.

We will continue to promote the best use of our research outcomes in various scientific and application areas. Our successes and achievements would not have been possible without the support of our valued partners. In this regard, I extend my thanks to you and I hope you enjoy this 2013 Research Report.

Chin-Seung Chung
Director, APEC Climate Center

CONTENTS

Construction of BSISO Forecast System and Application to Summer Monsoon Prediction

■■ Dr. Hae-Jeong Kim | Climate Analysis Team

APCC
RESEARCH REPORT 2013-02

Construction of BSISO Forecast System and Application to Summer Monsoon Prediction

Dr. Hae-Jeong Kim | Climate Analysis Team

ABSTRACT

The boreal summer intraseasonal oscillation (BSISO) is one of the dominant phenomena of summertime atmospheric variability in the tropics. The BSISO influences summer monsoon onsets and interacts with a wide range of atmospheric circulation patterns and associated weather. As the occurrence of and concern over extreme events rises, high-quality BSISO forecasts will become increasingly important.

The BSISO forecast service is now available at http://www.apcc21.org/eng/service/bsiso/fore/japcc030601.jsp, with contributions from four operation centers in cooperation with the WMO Commission for Atmospheric Sciences (CAS)/World Climate Research Program (WCRP) Working Group on Numerical Experimentation (WGNE) Madden Julian Oscillation (MJO) Task Force. The APCC BSISO forecasts are displayed in phase space using newly developed indices that represent BSISO activity with northward propagation over the off-equatorial monsoon domain.

From observations, the Changma onset may be influenced by the BSISO, which showed a northward propagating component about 20 days before the onset. Moreover, the development of strong and long Changma activity may be related to the summertime subtropical anticyclonic circulation over the western North Pacific and small convective anomalies to the north on an intraseasonal time scale.

1. INTRODUCTION

Recently, international attention on subseasonal forecasting has increased. The Subseasonal to Seasonal (S2S) Prediction Project and the World Weather Research Program (WWRP)/The Pbserving-System Research and Predictability Experiment (THORPEX)/World Climate Research Program (WCRP) joint research project have been set up to improve both forecasting skill and understanding of the subseasonal to seasonal timescale with a special emphasis on high impact weather. From an end-user perspective, the S2S is a very relevant time-scale for many management decisions in disaster risk reduction, water and agriculture, and food security. However, forecasting on the S2S timescale has been considered a “predictability desert” so far (Goswami et al., 2011; Kim et al., 2009; Waliser et al., 2006).

The intraseasonal oscillation (ISO), one of main issues for S2S prediction, can be an important potential source of predictability for subseasonal events (e.g., Vitart,

2013; Lee et al., 2010; Wang et al., 2009). In particular, the boreal summer ISO (BSISO), one of the dominant phenomena over the Asian summer monsoon region, has a large impact on extreme events and related disasters (Kikuchi and Wang, 2010). Therefore, the need for more accurate prediction of the BSISO has been emphasized. However, the BSISO has a lower predictability than the Madden-Julian Oscillation (MJO), since the propagation patterns of BSISO are considerably more complicated compared to boreal winter (Lee et al., 2013). Therefore, there have been several attempts to improve the predictability of BSISO (e.g., Lee et al., 2013; Wang et al., 2013; Sooraj and Seo, 2012).

The APEC Climate Center (APCC) has initiated forecasts of intraseasonal variability in order to keep up with this global issue. At the same time, the Working Group on Numerical Experimentation (WGNE) MJO Task Force, which initiated the monitoring and forecasting activity on the MJO in 2008 (Gottschalck et al., 2010), has been trying to extend this activity to the BSISO of the Asian monsoon region. Finally, since 2013, APCC has shared the forecast information of the BSISO in cooperation with the WGME MJO Task Force.

One of the most important impacts of the BSISO is its relationship with the summer monsoon (e.g., Moon et al., 2012; Wang et al., 2012; Wang and Xie, 1997). The impact of BSISO on the East Asia summer monsoon (EASM) is still unclear, although many studies have indicated the relationship due to the occurrence of high impact weather associated with monsoon onset and activity. Over the East Asia region (including Korea), much of the rainfall is from the summer monsoon. In Korea, the rainy season is called the Changma and it lasts from June to July. More than 30 percent of the annual precipitation falls during the Changma period (Figure 1). Variability of the BSISO can affect the onset, duration, and rainfall amount of the Changma, which is prominent on the intraseasonal time scale.

In this report, I describe the construction of the BSISO real-time forecast system, and investigate the relationship between the BSISO and the EASM, specifically the Changma, using composite analysis.

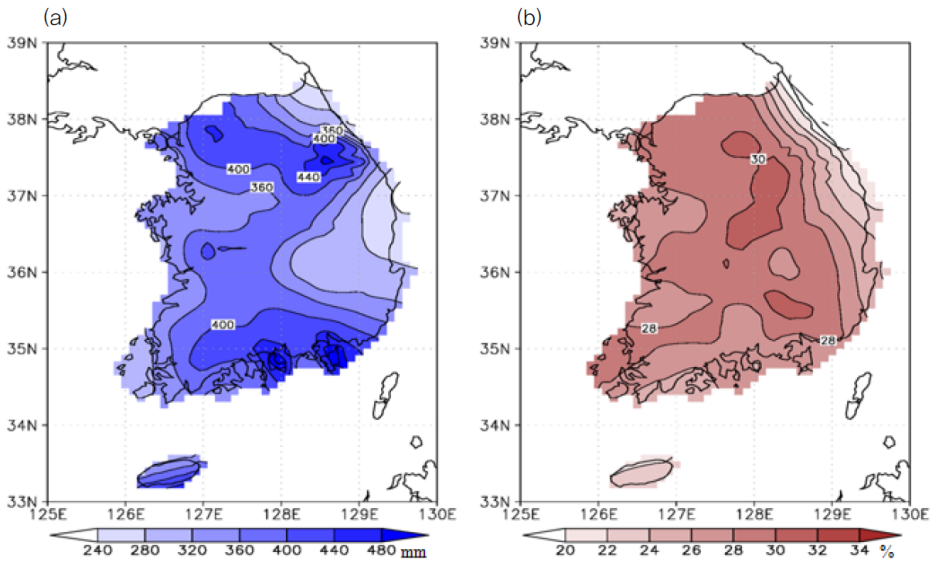

Figure 1 (a) Distribution of precipitation during the Changma period and (b) ratio of Changma rainfall to annual rainfall for the period 1981-2010 (Seo et al, 2011).

2. DATA AND METHODOLOGY

2.1 Data

The daily observation data was obtained from the National Centers for Environmental Prediction (NCEP)/Department of Energy (DOE) Reanalysis II (Kanamitsu et al., 2002). The daily Advanced Very High Resolution Radiometer (AVHRR) Outgoing Longwave Radiation (OLR) data were gathered from the National Oceanic and Atmospheric Administration (NOAA) polar orbiting satellites (Liebmann and Smith, 1996).

2.2 Methodology

2.1.1 BSISO Index

The new index of BSISO was developed by Lee et al. (2013) to overcome the limitation of representing BSISO over the off-equatorial monsoon domain. This index captures the northward propagating ISO that occurs in the Asian monsoon, as well as higher-frequency components exhibiting Rossby wave characteristics. In this study, the newly-developed BSISO index was used to isolate the BSISO signal from 1980 to 2010.

2.1.2 EASM

To examine the general relationship between the BSISO and EASM, concretely the Changma, the onset dates, durations, and precipitation amounts were obtained from a white paper on the Changma (KMA, 2011). Boreal summer was defined as June to July (JJ), covering the Changma period. The composite analysis was performed on the OLR and wind at 850 hPa during the period of 1980-2000. A Changma event was defined to have taken place if the magnitude of the index exceeded 0.5 standard deviations. For each variable, the mean and seasonal cycle were removed to generate anomalies. The running mean of the last 120 days was then subtracted for the removal of low frequency components (Lee et al., 2013; Gottschalck et al., 2010; Wheeler and Hendon, 2004). In this study, the anomalies were referred to as unfiltered data. The BSISO is known to have two major periods, at roughly 30-60 and 10-20 days, and to focus on these peaks, the data were filtered by applying a 30-60 and 10-20 day using Lanczos band pass filter (Duchon, 1979).

3. RESEARCH RESULTS

3.1 Construction of the BSISO real-time forecast system

3.1.1 Participating models and required forecast data

Table 1 shows the number of ensemble members, forecast period, update frequency, and resolution for each dataset used in the forecast. Four institutes, including NCEP, the Australian Bureau of Meteorology (BOM), the European Centre for Medium-Range Weather Forecasts (ECMWF) and the Met Office (UKMO), and five climate models from the MJO Working Group were included in this forecasting activity. The forecast durations varied, but only 20-day forecasts were released in this activity.

In order to participate in the activity, there were specific data needed from the operational centers (Table 2). The fields were latitudinally averaged OLR and zonal wind at 850 hPa for each model forecast day and for all ensemble members. Data were provided as daily mean with a 2.5-degree resolution in ASCII format. In addition, analysis data for the past 120 days were required at the beginning of the data transfer.

Table 1 Specific information for each of the current and planned data streams

Institute	Model	Ensemble Size	Forecast Period	Update Frequency	Resolution
NCEP	Climate Forecast System	4	40 days	Once per day	T126 L64
	Global Forecast System	1	16 days	Once per day	T574, T190 L64
BOM	POAMA 2.4 multi-week model	33	40 days	Twice per week	T47 L17
ECMWF	ECMWF Ensemble Prediction System	51	32 days	Twice per week	T639, T319 L62
UKMO	MOGREPS-15	24	15 days	Once per day	60km L70

Table 2 Specifications for the type and format of data needed from the operational centers

Fields	OLR, and U850 totals (anomaly fields optional)
Resolution	2.5° (10° S to 40° N and 40° to 160° E) Daily averaged (00-24Z)
Update Frequency	Daily preferred, but less for those systems run at a reduced frequency
Additional data	At beginning of transfer, send analysis data for past 120 days
Format	ASCII

3.1.2 Forecast procedure

The data were processed according to the procedure shown in Figure 2. Data were transferred by FTP in real time. The forecast anomalies were obtained by subtracting the mean and the first three harmonics of the seasonal cycle as calculated from the observed daily OLR and zonal wind at 850 hPa during 1981-2010. The running means of the last 120 days of model analysis/forecast anomalies were removed to subtract the effect of low frequency variability. Then, the forecast anomalies were divided by normalization factors and then projected onto the observed EOFs. The final product was a phase diagram displaying BSISO 1 and BSISO 2 values from the projection coefficients, including the values for the most recent 15 days and forecasts from the operational models for the next 20 days. The system automatically receives and processes the forecast data to produce the BSISO phase diagrams.

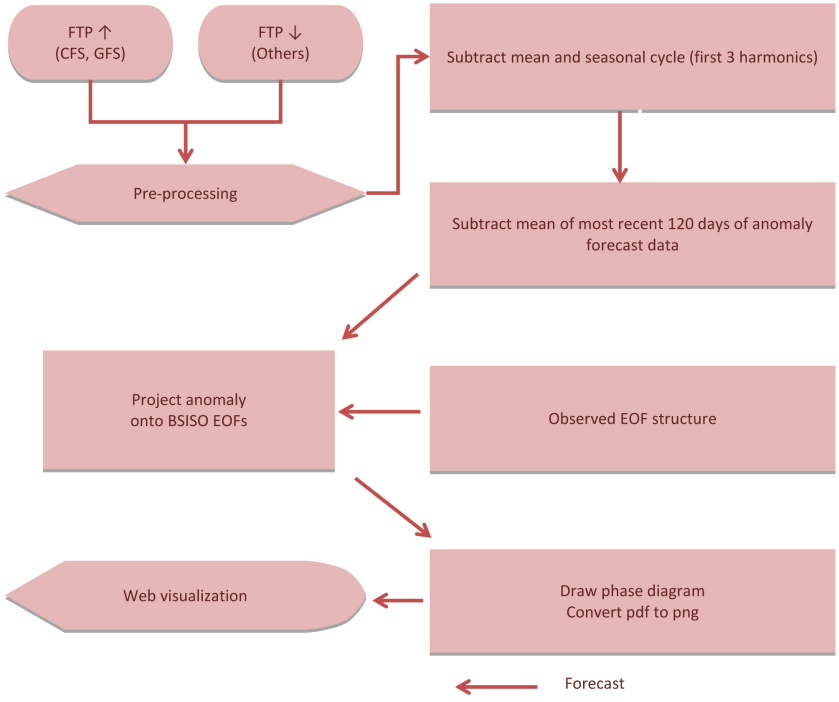

Figure 2 BSISO real time operational forecast system. The red arrow indicates the forecast procedure of the BSISO.

3.1.3 Forecast display and dissemination

Since June 2013, the BSISO forecasts have been provided in the form of phase diagrams on the APCC webpage at http://www.apcc21.org/ens/service/bsiso/fore/japcc030601.jsp (Figure 3). The BSISO forecast is updated every day with the latest information and is available from May to October.

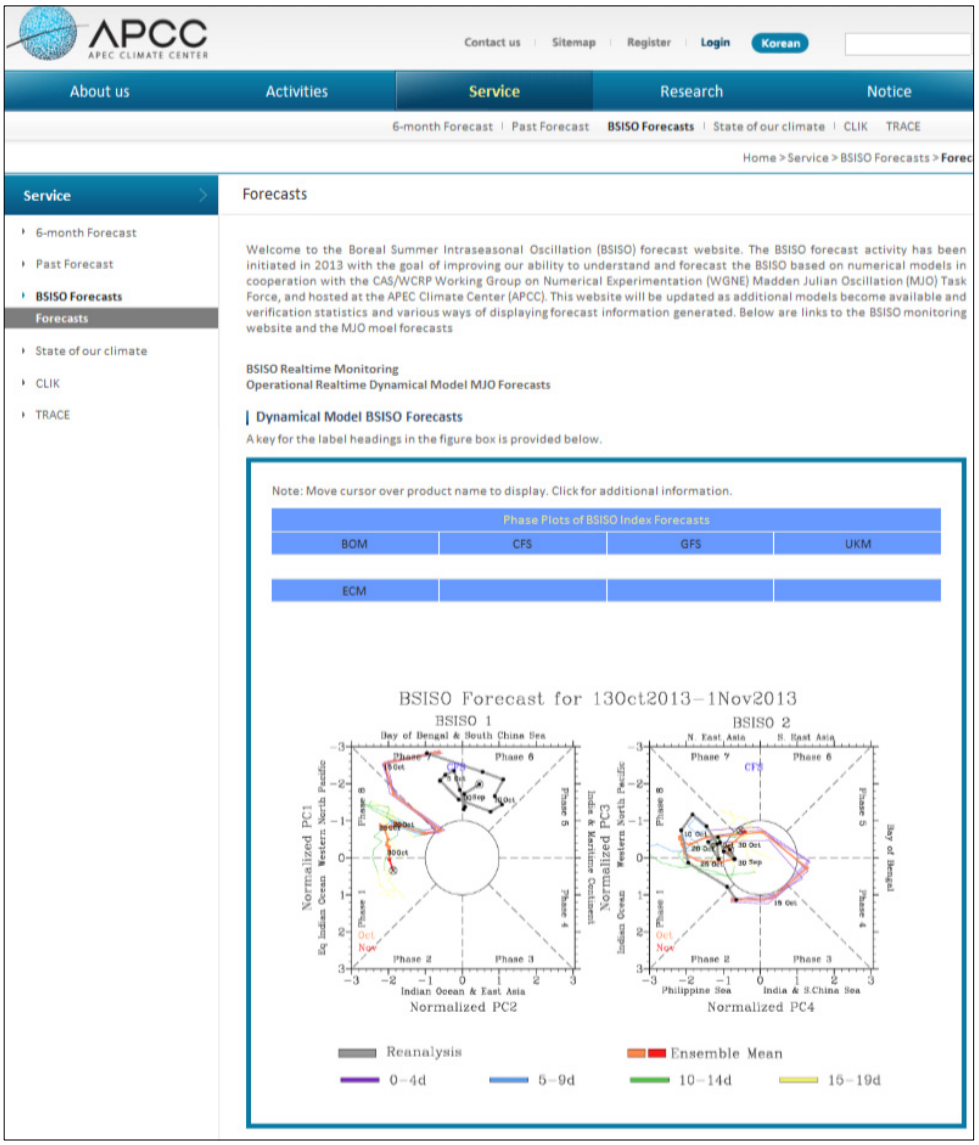

Figure 3 BSISO forecasts as they appear on the APCC webpage.

3.1.4 Issues and future plans

The following figures show three distinct examples of the BSISO real-time forecast as normal (Figure 4), backward (Figure 5) and standing oscillating cases (Figure 6). In this paper, I addressed the three phases of BSISO. The circulation characteristics and predictive skill of each example will be discussed in depth in a future paper after constructing a BSISO verification system.

3.1.4.1 Normal propagation

Figure 4 shows the normal propagation case for 14 October 2013 through 3 November 2013. Counterclockwise movement of daily points from phases 6 to 1 with an amplitude greater than 1 represents a typical event of the BSISO. Models showed similarities with one other but there were some differences in ensemble spread, propagation speed, and amplitude. In these phases, the convection over the South China Sea, associated with the cyclonic Rossby gyre over the Western North Pacific (WNP)-EA region, propagated northwestward with weakened amplitude (Lee et al., 2013).

3.1.4.2 Backward propagation

An example of a backward propagating case, indicated by clockwise rotation of the BSISO index, is shown in Figure 5. There were some differences between the centers in BSISO amplitude, propagation speed, and ensemble spread. The BSISO amplitude and propagation speed among the models were similar with a short lead-time. But there were considerable differences with increased lead time. Previous studies have shown that backward propagation is occasionally discerned in the phase space (e.g., Roundy et al., 2009; Zhang, 2006; Wheeler and Hendon, 2004; Hendon and Kiebmann, 1994; Nakazawa, 1988). The propagation can be caused by combining several higher-frequency small-scale convective systems moving in various directions (e.g., westward moving equatorial Rossby waves). It is also to be expected that the BSISO will display “backward” propagation more often, given that the coherence between the BSISO time series is less than that between the RMM time series (Lee et al., 2013; Wheeler and Hendon, 2004).

3.1.4.3 Standing oscillation

A standing phase oscillation is evident in the Figure 6. Most models displayed weak revolving tracks in phase 3 or 4 around the initial forecast day. In these phases, the northwest-southeast tilted convection was located along the Indian subcontinent to the Maritime continent (Lee et al., 2013). However, the reason for the standing oscillation needs further investigation.

To quantitatively evaluate this characteristic, we will construct a real-time BSISO verification system using metrics such as a bivariate correlation, root mean square error, and amplitude and phase error as shown in Gottschalck et al. (2010).

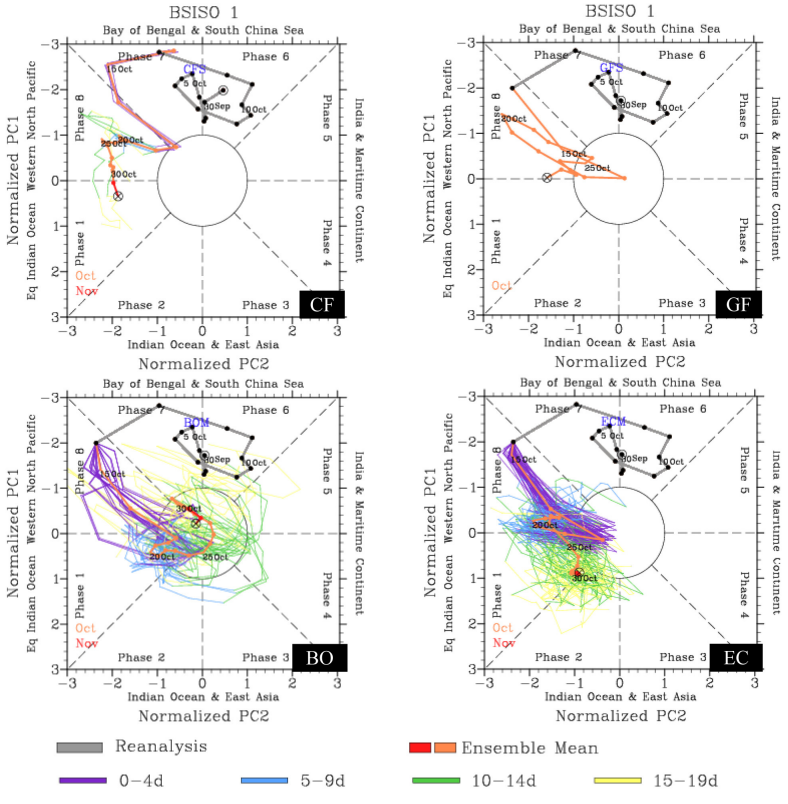

Figure 4 BSISO phase plots for 14 October-3 November 2013. The observations for the most recent 15 days (thick gray line) and forecasts for next 20 days (colored lines) are shown with the ensemble mean (thick red or orange line) and individual ensemble members (thin colored lines) in phase space.

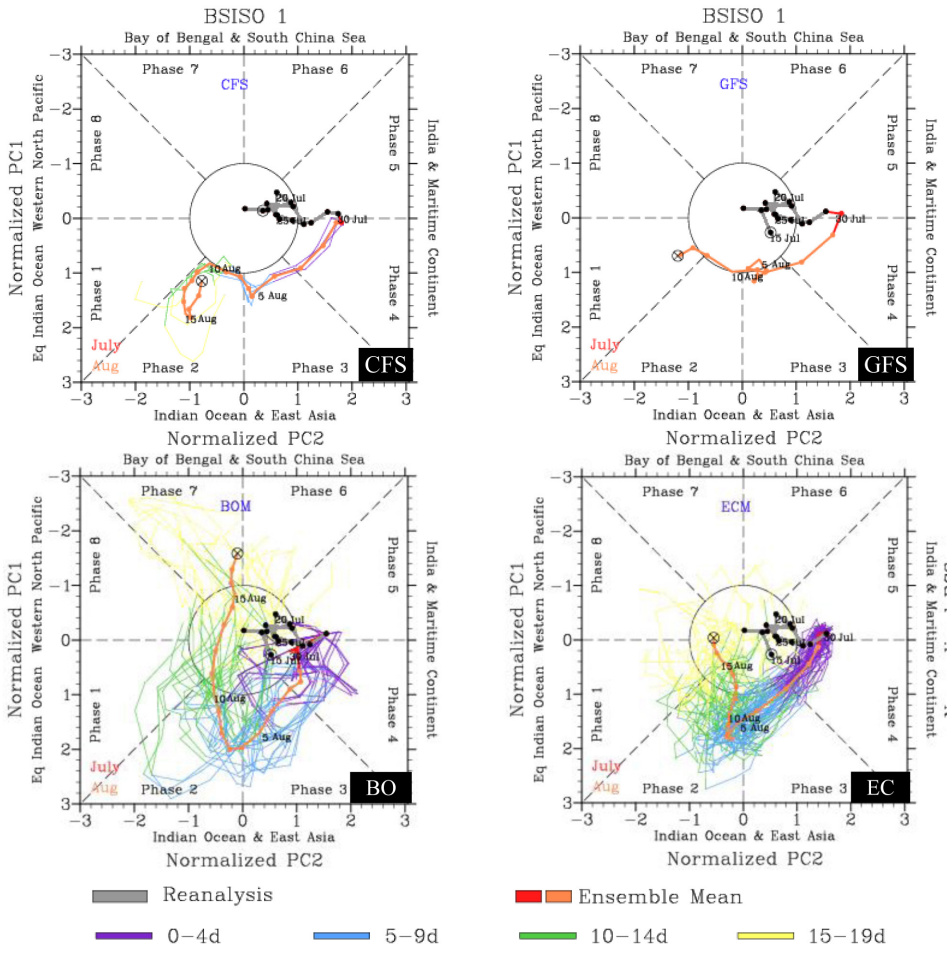

Figure 5 Backward movement occurred from 29 July through early August 2013.

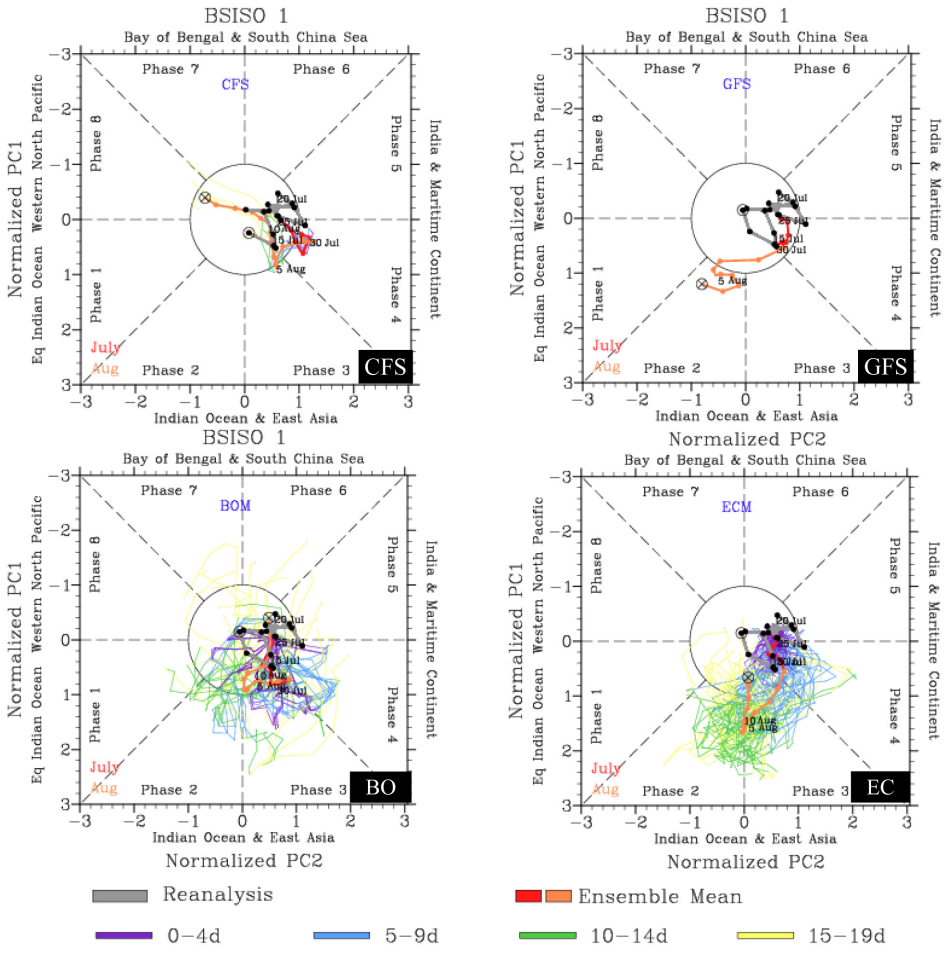

Figure 6 A standing oscillation occurred from 25 July through early August 2013.

3.2 Relationship between the BSISO and EASM

It has long been recognized that the BSISO plays a critical role in modulating the Asian summer monsoon, but the precise relationship has remained a persistent challenge. In this section, the relationship between the BSISO and the Changma is investigated using composite analysis. Composite analysis was performed by separating the BSISO and Changma indices. The strong, weak, and normal events of the BSISO

and those of Changma were categorized by thresholds of 1.5 and 0.5 standard deviations, respectively. In this study, boreal summer was defined as June to July (JJ), covering the Changma period. Therefore, the composite analysis was applied only for JJ.

3.2.1 Composite fields based on the BSISO indices

According to the BSISO indices defined by Lee et al. (2013), there were four BSISO indices comprising the first (BSISO 1-1), second (BSISO 1-2), third (BSISO 2-1) and fourth (BSISO 2-2) multivariate EOF modes. The number of days for strong and weak categories used in the composites is shown in Table 3. Figures 7-9 shows the differences in the composites between strong and weak BSISO events.

Table 3 Number of days in the strong and weak categories of the BSISO index during 1980-2010

	BSISO 1-1	BSISO 1-2	BSISO 2-1	BSISO 2-2
Strong days	148	112	136	92
Weak days	129	146	150	124

Figure 7 shows the difference in 5-day mean composites for OLR and 850 hPa wind vector anomalies based on the BSISO 1-1. When the event occurred, anomalous anticyclonic circulation was located over the subtropical western Pacific and subsequently weakened over time. Simultaneously, the anomalous southwesterly wind and convective activity that were present in the area south of the Korean peninsula propagated northward and enhanced during the 1-15 days after the event. Comparing the 30-60 and 10-20 day filtered anomalie, the influences of the BSISO on the EASM could be primarily explained by the 30-60 day filtered anomaly.

The composite differences based on the BSISO 1-2 (Figure 8) were consistent with the mature phase 4 of BSISO1 of Lee et al. (2013). The negative OLR anomaly and southwesterly wind anomaly were over Korea when the event started, and became more dominant about 5 days later (Figure 8). The anomalies then gradually disappeared after about 10 days. The 30-60 day filtered composite was more dominant compared to the 10-20 day filter.

Figure 9 shows the differences in the composite associated with BSISO 2-1. When the event started, the positive OLR anomalies and anomalous easterlies were dominant over Korea. The anomalies gradually weakened over time and then disappeared after 10 days. Based on this, the BSISO 2-1 is likely to have little impact on the precipitation in the northern East Asian region where our interest is on what occurred 20 days after the event began.

For BSISO 2-2, the westerlies covered a wide area and negative OLR anomalies extending east and west were evident in the southern Korean peninsula (Figure 10). The pattern gradually propagated northward and reached Korea after 15 days.

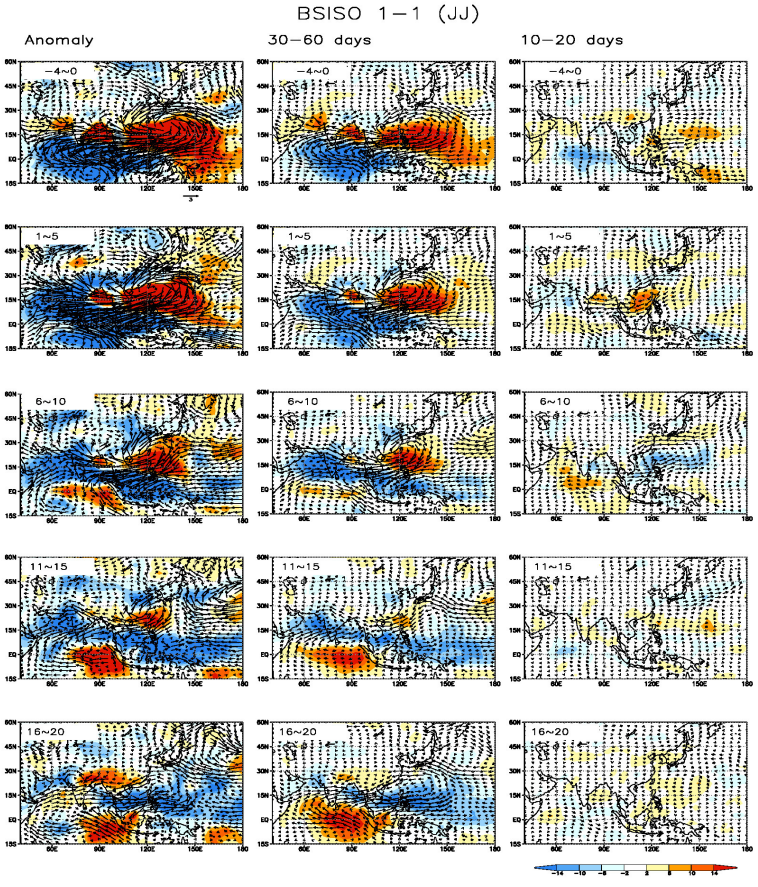

Figure 7 The 5-day mean composites of OLR anomalies (color) and 850 hPa wind vector anomalies (left), 30-60 (middle) and 10-20 (right) day filtered anomalies based on BSISO 1-1 during June-July.

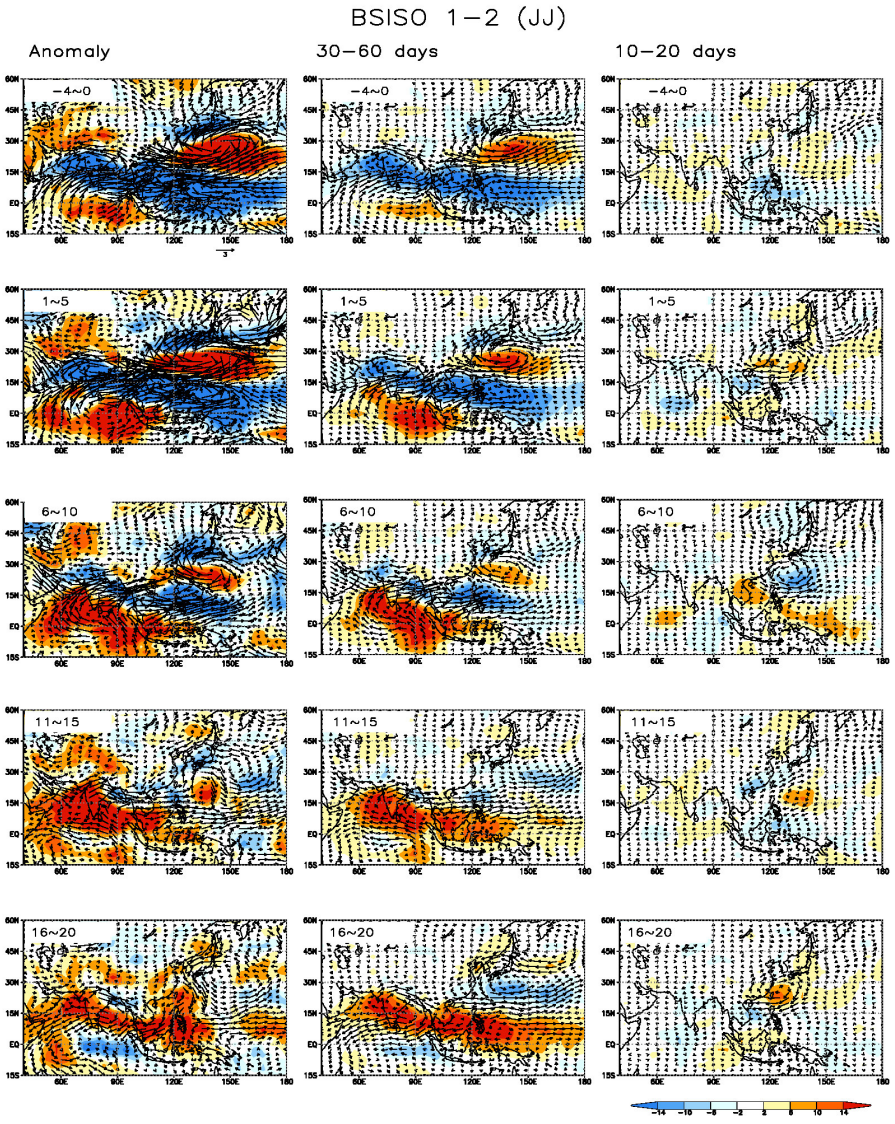

Figure 8 Same as Figure 7 except for BSISO 1-2.

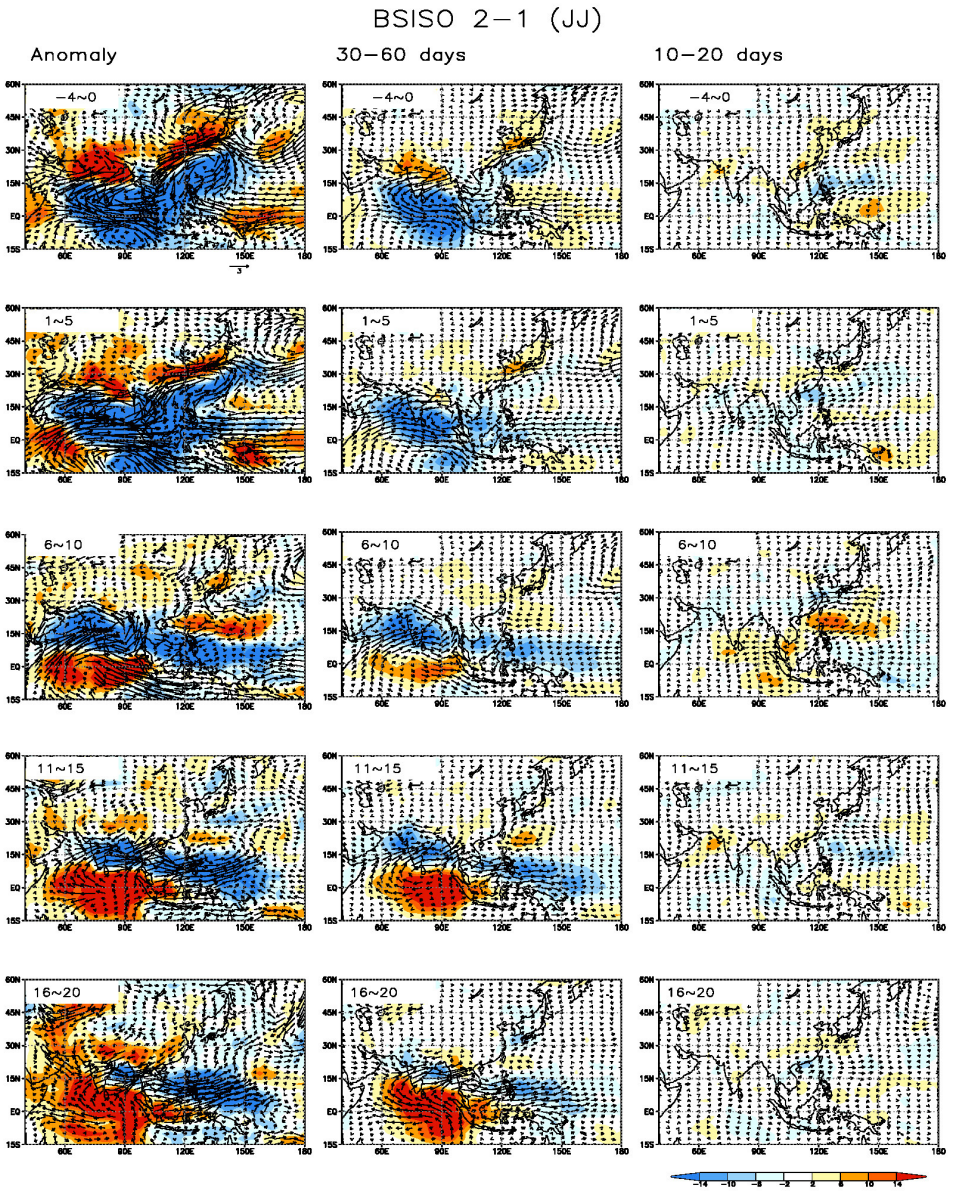

Figure 9 Same as Figure 7 except for BSISO 2-1.

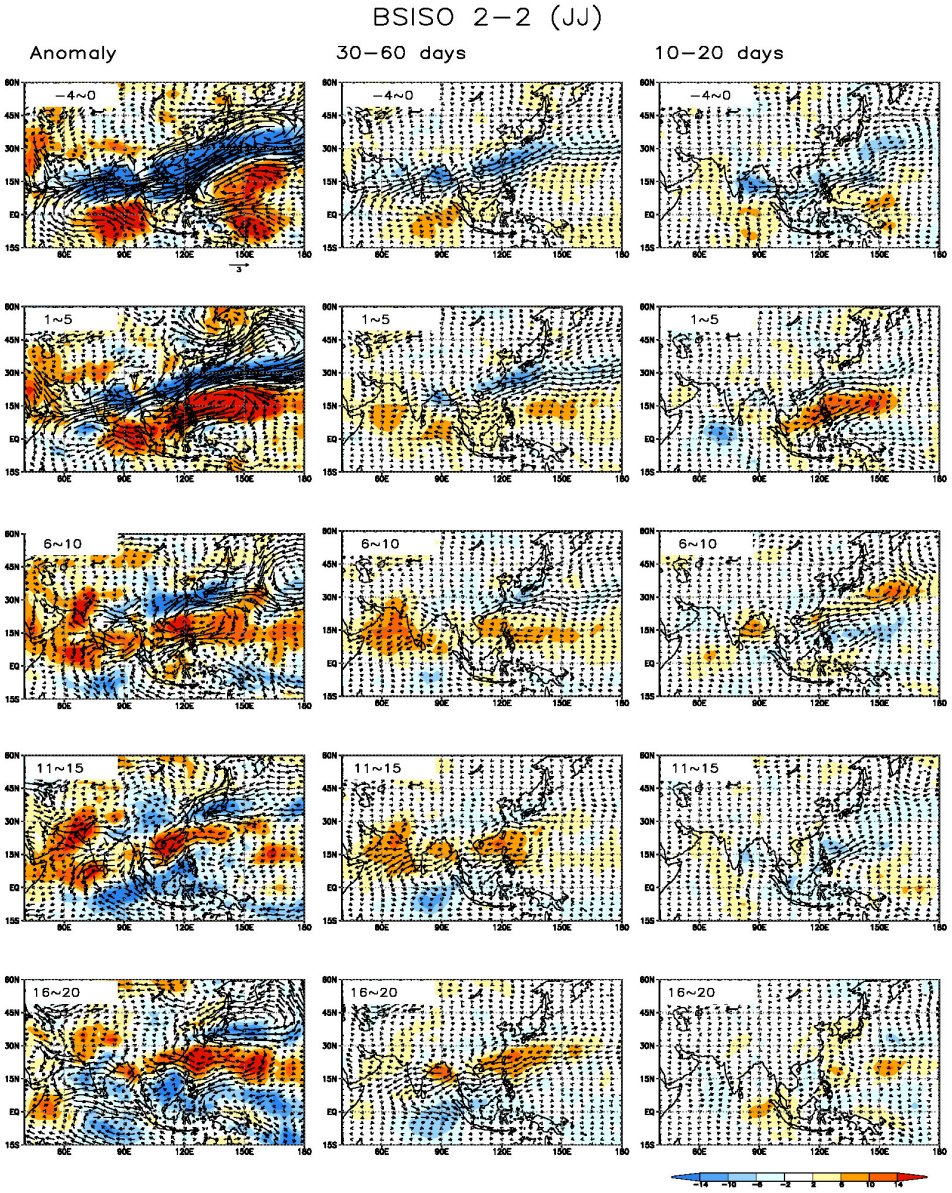

Figure 10 Same as Figure 7 except for BSISO 2-2.

3.2.2 Composite anomalies associated with the Changma indices

In this section, the Changma is characterized by the precipitation onset, duration, and strength.

3.2.2.1 Onset

The Changma onset dates identified in this study are shown in Table 4. The mean onset date was 23 June for the 30 year period (KMA, 2011). The 0.5 standard deviation was 5.3 days.

Figure 11 shows the time-latitude diagram for the OLR anomalies over 115°-140° E. For the three onset cases, northward propagation from 15° N to approximately 30° N was evident and in most cases was explained by the 30-60 day filtered anomaly. It also showed that the Changma could be influenced by the BSISO within about 20 days of the onset. The 10-20 day filtered OLR also propagated from the equator to approximately 30° N during the 20 days before the late onset. The late onset involved the impact of both 30-60 day and 10-20 day variability. On the other hand, the 10-20 day oscillation showed southward movement from north of 15° N before the early onset but did not affect the Changma onset directly.

The above relationships (Figure 11) were also seen in the 5-day mean composite OLR and low-level wind anomaly maps for the Changma onset case (Figure 12). For the late onset, negative OLR anomalies and westerly anomalies caused by the anomalous anticyclonic circulation located at 15°-30° N, 110°-150° E were seen over Korea during onset period. From 20 days before late onset, the OLR anomalies extending from 15° to 30° N and 120° to 150° E propagated northwestward to Korea. For the early onset, the negative OLR anomalies over the western North Pacific and the edge of the anomalous anticyclonic circulation located at 120° E were favorable for moisture transport to Korea during onset. At 5 days before the onset, the dry northeasterly wind blew across Korea in the late onset case, preventing moisture from moving into the Korean peninsula, while the southwesterly wind supported the movement of more moisture into Korea during the early onset event.

Table 4 Onset dates of the Changma

Early years	Late years	Normal years
1981/06/19	1982/07/07	1985/06/21
1983/06/19	1987/07/01	1986/06/22
1984/06/15	1991/06/26	1988/06/23
1990/06/19	1992/07/09	1989/06/23
1997/06/20	1995/06/30	1993/06/22
1999/06/17	2005/06/26	1994/06/22
2008/06/17		1996/06/24
2010/06/18		1998/06/24
		2000/06/21
		2001/06/22
		2002/06/23
		2003/06/23
		2004/06/24
		2006/06/21
		2007/06/21
		2009/06/21
8	6	16

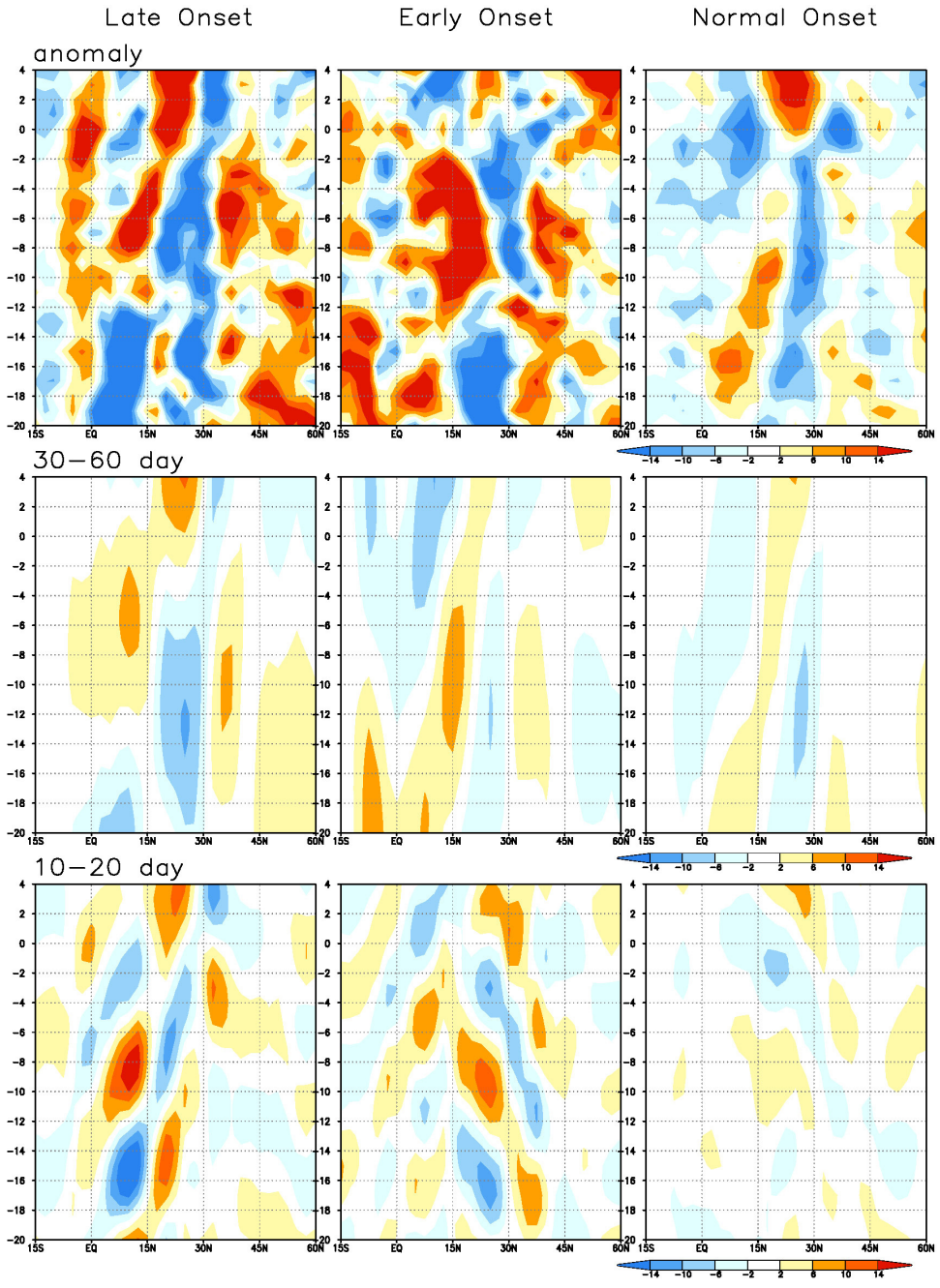

Figure 11 Hovmoller diagram of OLR composite anomalies based on the Changma onset.

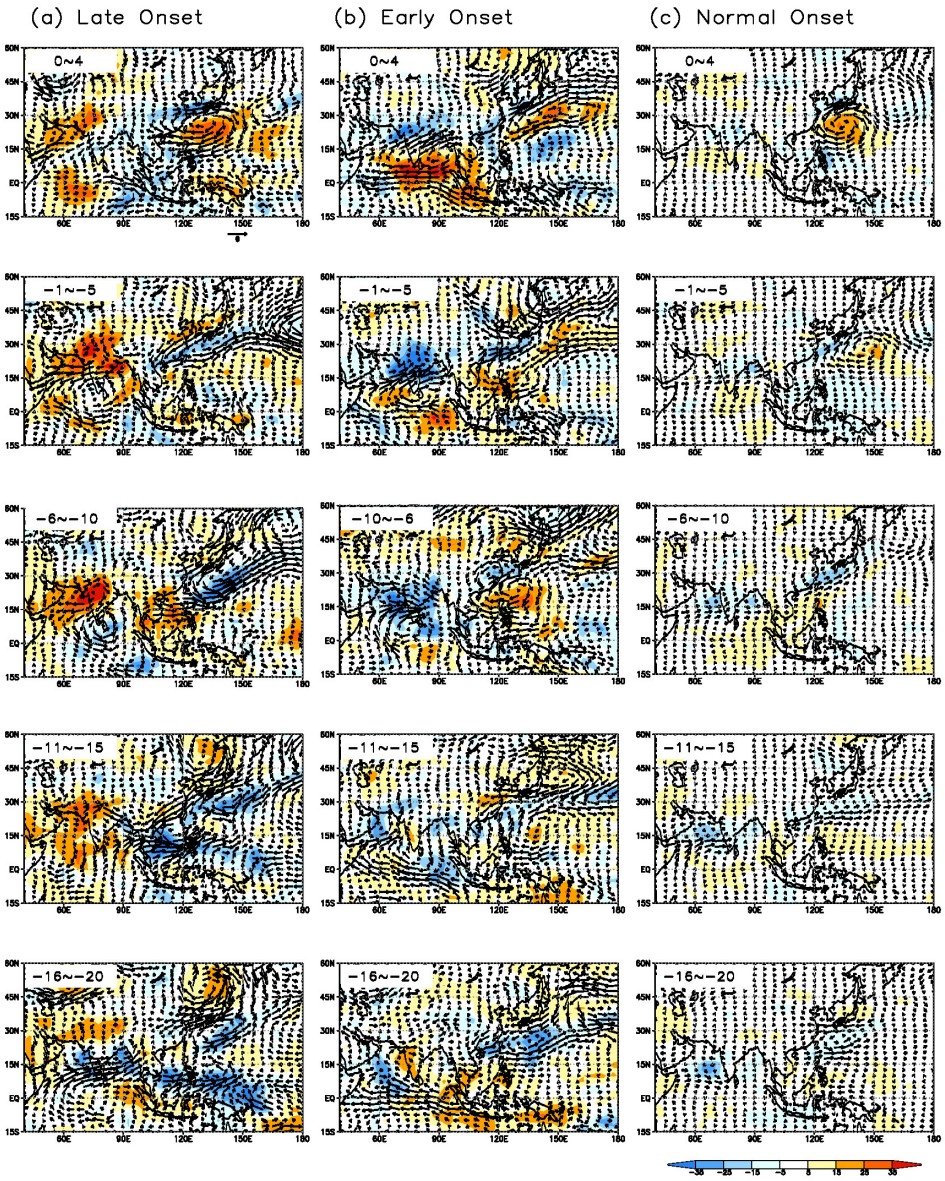

Figure 12 Composite OLR and 850 hPa wind anomalies based on the Changma onset.

3.2.2.2 Duration

Table 5 shows the duration of the Changma. The mean Changma duration was 31 days over the 30 year period (KMA, 2011). The 0.5 standard deviations for the Changma duration was 7 days.

Figure 13 shows the time evolution of the convective and circulation anomalies associated with the Changma duration. For the long duration case, moisture was transported northward or northeastward into Korea along the western edge of the anticyclonic anomaly located in 120° E, and appeared likely to converge with Korea. The circulation covered a wide range over the North Pacific from 120° to 180° E. This structure could continuously deliver the warm and moist air to the Korean peninsula, resulting in a long Changma duration.

For the short duration case, a considerably shrunk anomalous anticyclonic circulation appeared in southern Korea and the western edge of the anticyclonic anomaly was shifted to interior China. The wind speed also intensified in this case. This structure could supply more dry and warm air to Korea, leading to a short Changma duration.

These characteristics appeared to be more related to the 30-60 day intraseasonal variability.

Table 5 Duration of the Changma

Short duration years (day)	Long duration years (day)	Normal duration years (day)
1981 (26)	1983 (36)	1984 (29)
1982 (23)	1987 (39)	1985 (28)
1992 (15)	1989 (37)	1986 (34)
1994 (15)	1991 (38)	1988 (35)
2000 (26)	1993 (39)	1990 (31)
2004 (24)	2006 (39)	1995 (28)
2005 (23)	2008 (40)	1996 (29)
	2009 (44)	1997 (29)
	2010 (41)	1998 (35)
		1999 (34)
		2001 (30)
		2002 (31)
		2003 (33)
		2007 (34)
7	9	14

3.2.2.3 Strength

Table 6 shows the precipitation amount during the Changma period. The mean precipitation was 306 mm/day over the 30-years period (KMA, 2011). The 0.5 standard deviation for Changma strength was 131.6 mm/day.

Figure 14 shows the composite map based on the Changma precipitation amount. The anomalous anticyclonic wind anomalies over Korea were stronger during heavier precipitation than they were during lighter precipitation. In the heavy precipitation case, the strong southerly wind pushed more moisture toward Korea than during the lighter precipitation case. In the 30-60 day filter, the dry anomalous northwesterly air seemed to blow over Korea, as well as southwesterly winds during lighter precipitation events, resulting in below normal precipitation. The anomalies related to the Changma precipitation amount appeared to reflect the 30-60 day filtered composite.

Overall, it can be understood that the development of strong and long Changma activity was mainly related to the summertime WNP subtropical anticyclonic circulation as well as small convective anomalies to the north.

Table 6 Rainfall amount during the Changma period

Lowest years	Higheast years	Normal years
1982 (212.0)	1985 (511.2)	1981 (346.8)
1992 (162.7)	1987 (512.1)	1983 (339.1)
1994 (73.2)	1989 (441.1)	1984 (358.8)
1995 (176.6)	1991 (447.6)	1986 (393.7)
1999 (270.4)	1997 (470.9)	1988 (312.5)
2000 (288.5)	2003 (585.4)	1990 (420.8)
2002 (281.5)	2006 (653.2)	1993 (361.7)
2004 (258.9)	2009 (614.7)	1996 (334.1)
2005 (284.3)		1998 (415.4)
		2001 (336.0)
		2007 (300.5)
		2008 (324.5)
		2010 (340.5)
9	8	13

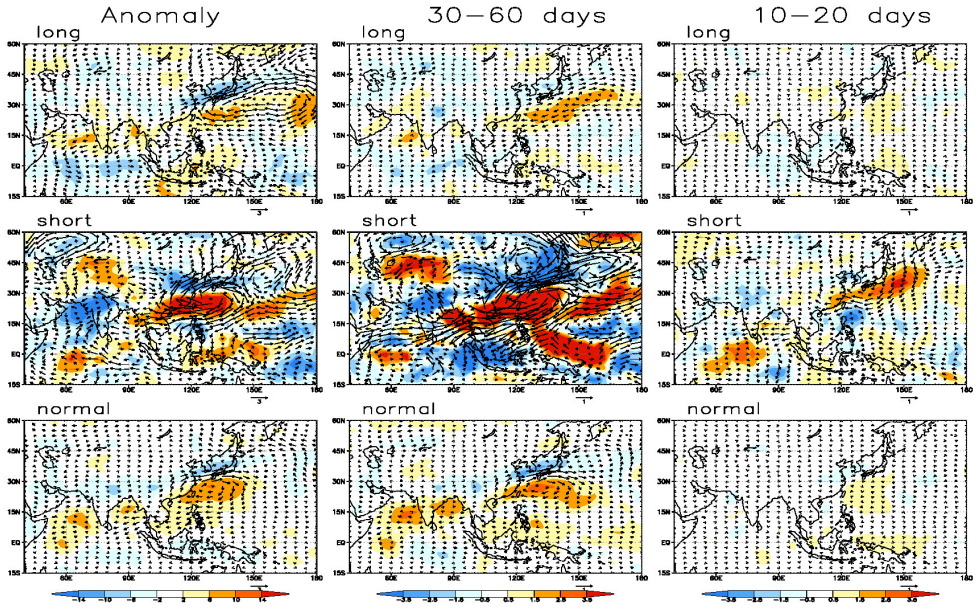

Figure 13 Composite OLR and 850 hPa wind anomalies based on the Changma duration.

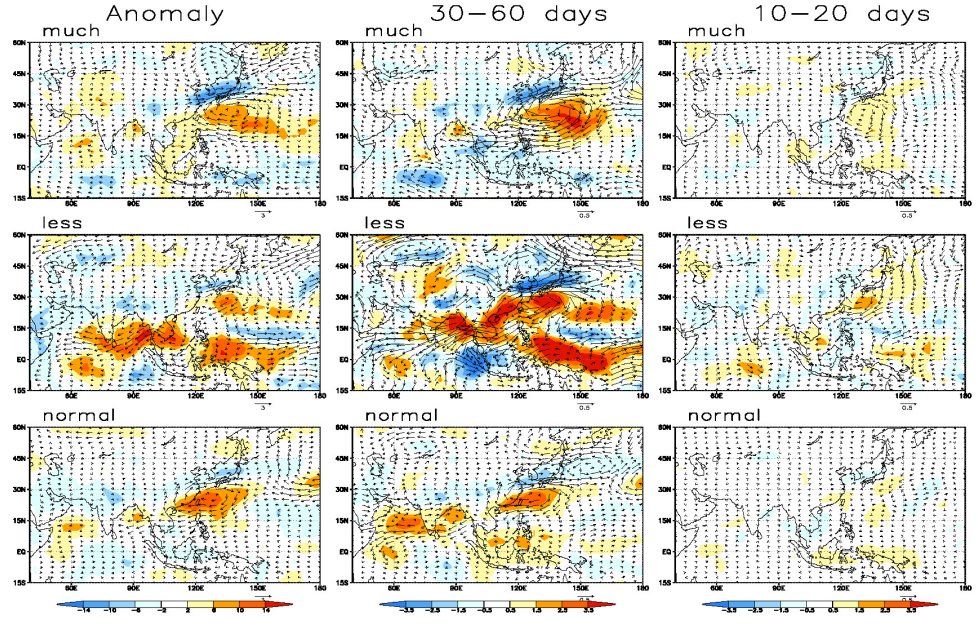

Figure 14 Same as Figure 13, except for the Changma precipitation amount.

4. CONCLUDING REMARKS

The BSISO is one of the dominant phenomena of summertime atmospheric variability in the tropics. The BSISO influences summer monsoon onsets (e.g., Wang and Xie, 1997) and interacts with a wide range of atmospheric circulation patterns and associated weather (e.g., Lee et al., 2011; Wang et al., 2012). In addition, the wet and dry spells of the BSISO can strongly influence extreme hydro-meteorological events, major driving forces of natural disasters (Lau and Waliser, 2005). As the occurrence of and concern over extreme climate events rises, providing high-quality BSISO forecasts will become increasingly important. The objectives of this study were to construct a real-time BSISO forecast system and to address the relationship between the BSISO and EASM, especially the Changma.

APCC has recently begun to provide the BSISO forecast information service at http://www.apcc21.org/eng/service/bsiso/fore/japcc030601.jsp, with contributions from the BOM, the US NCEP, the ECMWF and UK Meteorology Office in cooperation with the CAS/WCRP Working Group on Numerical Experimentation Madden Julian Oscillation Task Force. The APCC BSISO forecasts are displayed by newly developed indices proposed by Lee at al. (2013) that represent BSISO activity with northward propagation over off-equatorial monsoon domain. Based on this work, we also expect to provide a real-time verification service of BSISO on the APCC web page. In hosting the BSISO forecasting activity, APCC has made a valuable contribution by providing forecast information based on the BSISO multi-model prediction system and suggesting models that potentially have the capability to capture the BSISO. This also establishes the foundation for BSISO Multi-Model Ensemble forecasts based on these models. The participation of additional forecast centers will be essential to promote this forecasting activity.

Although this study did not specifically explain how the BSISO could influence on the Changma, it might contribute to the understanding of the relationship and provided the foundation for further study. Each of the cases for the onset, duration, and strength of the Changma (strong, weak, and normal) were related to phase 5 for both BSISO1 and BSISO2. The Changma onset could be influenced by the BSISO

with a northward propagating component about 20 days before the onset. Moreover, the development of strong and long Changma activity could be related to the summertime WNP subtropical anticyclonic circulation as well as small convective anomalies to the north on the intraseasonal time scale. Further studies in the next year will clarify these relationships with significance testing using various atmospheric variables to investigate possible mechanisms.

This research is expected to improve our understanding of the BSISO and its teleconnection. The BSISO forecast information may also be useful for predicting summer monsoon onset and activity over the East Asia region, helping to mitigate the agricultural and socioeconomic impacts of natural disasters.

REFERENCES

Duchon, C.E., 1979: Lanczos filtering in one and two dimensions. *J. Appl. Meteor.,* **18,** 1016-1022.

Goswami, B.N., M.C. Wheeler, J.C. Gottschalck, and D.E. Waliser, 2011: Intraseasonal variability and forecasting: a review of recent research. *The Global Monsoon System: Research and Forecast, 2nd edition* C.-P. Chang, Y. H. Ding, N.-C. Lau, R. Johnson, B. Wang, and T. Yasunari, Eds., World Scientific Series on Asia-Pacific Weather and Climate, 5, 389-408.

Gottschalck, J., M. Wheeler, K. Weickmann, F. Vitart, N. Savage, H. Lin, H. Hendon, D. Waliser, K. Sperber, M. Nakagawa, C. Prestrelo, M. Flatau, and W. Higgins, 2010: A framework for assessing operational Madden-Julian Oscillation forecasts: a CLIVAR MJO Working Group project. *Bull. Amer. Meteor. Soc.,* **91,** 1247-1258.

Hendon, H. H., and B. Liebmann, 1994: Organization of convection within the Madden-Julian Oscillation. *J. Geophys. Res.,* **99,** 8073-8083.

Kim, D., et al., 2009: Application of MJO simulation diagnostics to climate models. *J. Climate,* **22,** 6413-6436.

Kikuchi, K., and B. Wang, 2010: Formation of tropical cyclones in the northern Indian Ocean associated with two types of tropical intraseasonal oscillation modes. *J. Meteor. Soc. Japan,* **88,** 3, 475-496.

KMA, 2011: The Changma (white paper).

Lee, J. Y., B. Wang, I. S. Kang and J. Shukla et al., 2010: How are seasonal prediction skills related to models' performance on mean state and annual cycle? *Climate Dyn.,* **35,** 267-283.

Liebmann, B., and C. A. Smith, 1996: Description of a complete (interpolated) outgoing longwave radiation dataset. *Bull. Amer. Meteor. Soc.,* **77,** 1275-1277.

Ling, J., C. Zhang, and P. Bechtold, 2013: Large-scale distinctions between MJO and non-MJO convective initiation over the tropical Indian Ocean. *J. Atmos. Sci.,* **70,** 2696-2712.

Majda, A. J., and S. N. Stechmann, 2011: Nonlinear dynamics and regional variations in the MJO skeleton. *J. Atmos. Sci.,* **68,** 3053-3071.

Moon, J.-Y., B. Wang, K.-J. Ha, and J.-Y. Lee, 2012: Teleconnections associated with Northern Hemisphere summer monsoon intraseasonal oscillation. *Climate Dyn.,* doi:10.1007/s00382-012-1394-0.

Nakazawa, T., 1988: Tropical super clusters within intraseasonal variations over the western Pacific. *J. Meteor. Soc. Japna.,* **66,** 823-836.

Roundy, P., J. R. Kravitz, C. J. Schreck III, and M. A. Janiga, 2009: Contributions of convectively coupled equatorial Rossby waves and Kelvin waves to the real-time multivariate MJO indices. *Mon. Wea. Rev.,* **137,** 469-478.

Seo, K.-H., J.-H. Shon, and J.-Y. Lee, 2011: A new look at Changma (in Korean with English abstract). *Atmosphere,* **21,** 109-121.

Sooraj, K. P., and K.-H. Seo, 2013: Boreal summer intraseasonal variability simulated in the NCEP climate forecast system: insights from moist static energy budget and sensitivity to convective moistening. *Climate Dyn.,* DOI 10.1007/s00382-012-1631-6.

Vitart, F., 2013: Evolution of ECMWF sub-seasonal forecast skill scores. *Q. J. R. Meteor. Soc.,* DOI: 10.1002/qj.2256.

Waliser, D., K. Weickmann , R. Dole, S. Schubert, O. Alves, C. Jones, M. Newman, H.-L. Pan, A. Roubicek, S. Saha, C. Smith, H. van den Dool, F. Vitart, M. Wheeler, and J. Whitaker, 2006: The experimental MJO prediction project. *Bull. Amer. Meteor. Soc.,* **87,** 425-431.

Wang, B., and X. Xie, 1997: A model for the boreal summer intraseasonal oscillation. *J. Atmos. Sci.,* **54,** 72-86.

Wang, B., J. Y. Lee, J. Shukla, and I. S. Kang et al., 2009: Advance and prospectus of seasonal prediction: assessment of APCC/CliPAS 14-model ensemble retrospective seasonal prediction (1980-2004). *Climate Dyn.,* **33,** 93-117.

Wang, H., B. Wang, F. Huang, Q. Ding, J.-Y. Lee, 2012: Interdecadal change of the boreal summer circumglobal teleconnection (1958-2010). *Geophys. Res. Lett.,* **39,** L12704, doi:10.1029/2012 GL052371.

Wang, L., T. Li, T. Zhou and X. Rong, 2013: Origin of the intraseasonal variability over the North Pacific in boreal summer. *J. Climate,* **26,** 1211-1229.

Wheeler, M. C., and H. H. Hendon, 2004: An all-season real-time multivariate MJO index: development of an index for monitoring and prediction. *Mon. Wea. Rev.,* **132,** 1917-1932.

Zhang, C., 2005: Madden-Julian Oscillation. *Rev. Geophys.,* **43,** RG2003, doi:10.1029/2004RG000158.

APCC RESEARCH REPORT 2013-02

- Construction of BSISO Forecast System and Application to Summer Monsoon Prediction
- Revision of Climate Change by Dynamic Downscaling over the Maritime Continents
- Long-Lead Station-Scaled Prediction of a Hydrological Drought in South Korea Based on Bivariate Downscaling
- Development of Scaled SVD Analysis and Related Methods with Focus on Application to Tropical-Extratropical Teleconnections

APEC Climate Center

12, Centum 7-ro, Haeundae-gu, Busan 612-020,
Republic of Korea
Tel: +82-51-745-3900 Fax: +82-51-745-3949
www.apcc21.org

비매품
94550
9 788997 333943
ISBN 978-89-97333-94-3
ISBN 978-89-97333-92-9 (세트)